CANCER

# Reprogramming normal human epithelial tissues to a common, lethal neuroendocrine cancer lineage

Jung Wook Park[1], John K. Lee[2], Katherine M. Sheu[3], Liang Wang[1], Nikolas G. Balanis[3], Kim Nguyen[4], Bryan A. Smith[1], Chen Cheng[5], Brandon L. Tsai[1], Donghui Cheng[1], Jiaoti Huang[6], Siavash K. Kurdistani[5,7,8,9], Thomas G. Graeber[3,7,8,9,10]*, Owen N. Witte[1,3,7,8,9]*

**The use of potent therapies inhibiting critical oncogenic pathways active in epithelial cancers has led to multiple resistance mechanisms, including the development of highly aggressive, small cell neuroendocrine carcinoma (SCNC). SCNC patients have a dismal prognosis due in part to a limited understanding of the molecular mechanisms driving this malignancy and the lack of effective treatments. Here, we demonstrate that a common set of defined oncogenic drivers reproducibly reprograms normal human prostate and lung epithelial cells to small cell prostate cancer (SCPC) and small cell lung cancer (SCLC), respectively. We identify shared active transcription factor binding regions in the reprogrammed prostate and lung SCNCs by integrative analyses of epigenetic and transcriptional landscapes. These results suggest that neuroendocrine cancers arising from distinct epithelial tissues may share common vulnerabilities that could be exploited for the development of drugs targeting SCNCs.**

Human cancers originating in different organs share commonalities in cancer phenotypes and molecular features (*1*). Small cell neuroendocrine carcinoma (SCNC) is recognized by its distinctive histological features and can arise from almost all epithelial organs, including the prostate and lung (*2*, *3*). These cancers show notable lineage plasticity and acquire therapeutic resistance by converting from an epithelial to a neuroendocrine cancer phenotype (*4*–*8*). Large-scale analyses of transcriptome data from a variety of cancer types have provided substantial evidence (*9*–*11*) to support a phenotypic convergence to SCNC during cancer progression. The underlying molecular mechanisms are not fully understood.

To explore whether distinct human epithelial cell types can be transformed into SCNC by shared oncogenic drivers, we used a human tissue transformation assay (*12*). Small cell prostate cancer (SCPC) is a type of neuroendocrine prostate cancer (NEPC), a class of malignancies that includes the extremely rare "large cell prostate carcinoma," whose exact definition is still emerging (*13*). Overexpression of c-Myc or N-Myc in combination with myristoylated AKT1 (myrAKT1) (a partial mimic of *PTEN* loss) drives normal human prostate epithelial cells to poorly differentiated prostate adenocarcinoma (PrAd) or SCPC, respectively (*12*, *14*). To identify additional oncogenic drivers of SCPC, we investigated the functional effects of dominant negative p53 (TP53DN) (P), myrAKT1 (A), *RB1*–short hairpin RNA (shRNA) (R), c-Myc (C), and BCL2 (B) on the genesis of SCPC on the basis of their recurrent genetic alterations in prostate cancers, including SCPC (*5*, *7*, *15*, *16*). These five genetic factors are hereafter referred to as PARCB. Primary basal epithelial cells were isolated from the prostates of eight human donors and were lentivirally transduced with the PARCB factors, briefly cultured in an organoid system (Fig. 1A), and transplanted into immunodeficient NOD/SCID-IL2R-γc-KO mice (*17*), where they formed tumors that displayed green, red, and yellow fluorescent protein (GFP, RFP, and YFP) expression from the three lentiviruses (Fig. 1B). PARCB gene expression and the human cellular origin of the tumors were confirmed by immunostaining (fig. S1). All PARCB tumors derived from basal cells demonstrated histological features of human SCPC, including a high nuclear-to-cytoplasmic ratio, frequent mitotic and apoptotic figures, and uniform expression of neuroendocrine differentiation (NED) markers (Fig. 1, C and D).

We next defined the genetic factors required to initiate SCPC from the PARCB combination by leave-one-out analysis. No tumors developed in the absence of either c-Myc or myrAKT1. In the absence of BCL2, the PARC combination still produced tumors with histologic characteristics and NED marker expression consistent with SCPC (Fig. 1D and fig. S2A), albeit with reduced efficiency (fig. S3). In contrast to BCL2, *RB1*-shRNA and TP53DN together or individually were indispensable for SCPC development. Tumors arising from these conditions—PACB (without *RB1*-shRNA), ARCB (without TP53DN), and ACB (without TP53DN and *RB1*-shRNA)—displayed histological features of poorly differentiated PrAd. PACB and ARCB tumors displayed only focal expression of NED markers (Fig. 1D). Thus, loss of *RB1* and inactivation of p53 are required to convert an epithelial lineage into a neuroendocrine lineage in SCPC development during human prostate epithelial transformation.

To further investigate the molecular contributions of the PARCB genetic factors to SCPC, we established tumor cell lines from fluorescence-activated cell sorting (FACS)–purified cells of the ACB, PACB, ARCB, and PARCB tumors (Fig. 2A). Immunoblot analysis confirmed the expression of the respective genetic factors in the newly generated cell lines (fig. S2B). We then performed two downstream global analyses: mRNA sequencing (RNA-seq) and assay for transposase-accessible chromatin sequencing (ATAC-seq). Currently, gene expression datasets specific for SCPC are lacking. We used the largest available RNA-seq dataset of NEPC and PrAd patient samples (*8*) in our study. We simplified the nomenclature of NEPC as SCPC to prevent confusion when alternating between epithelial tissue types.

Our RNA-seq data revealed that the PARCB cell lines have transcriptomes that are distinct from those characterizing ACB, PACB, and ARCB lines (fig. S4A), supporting the histologic and molecular differences described above. The PARCB cell lines exhibited enriched expression of genes that are up-regulated in clinical SCPC specimens relative to PrAd samples (*8*, *18*), whereas the ACB, PACB, and ARCB lines did not (fig. S5A). The PARCB lines were also highly similar to human SCPC (fig. S5B) on the basis of a published SCPC gene expression signature (*7*).

Global transcriptome analysis revealed that the PARCB cell lines exhibited strong transcriptional similarity to SCPC patient samples, whereas the other engineered cell lines clustered with patient-derived PrAd cell lines (Fig. 2B). They did not express detectable levels of androgen receptor (AR) and exhibited the lowest level of AR signaling activity when compared with clinical samples (fig. S6). The PARCB cell lines also exhibited NED markers in vivo and in vitro (fig. S7).

Open- or closed-chromatin regions can be indicative of transcriptional regulatory elements and serve as predictors of gene transcription activity. We measured genome-wide chromatin

[1]Department of Microbiology, Immunology, and Molecular Genetics, University of California–Los Angeles, Los Angeles, CA 90095, USA. [2]Division of Hematology and Oncology, Department of Medicine, University of California–Los Angeles, Los Angeles, CA 90095, USA. [3]Department of Molecular and Medical Pharmacology, University of California–Los Angeles, Los Angeles, CA 90095, USA. [4]Department of Ecology and Evolutionary Biology, University of California–Los Angeles, Los Angeles, CA 90095, USA. [5]Department of Biological Chemistry, University of California–Los Angeles, Los Angeles, CA 90095, USA. [6]Department of Pathology, School of Medicine, Duke University, Durham, NC 27710, USA. [7]Molecular Biology Institute, University of California–Los Angeles, Los Angeles, CA 90095, USA. [8]Jonsson Comprehensive Cancer Center, University of California–Los Angeles, Los Angeles, CA 90095, USA. [9]Eli and Edythe Broad Center of Regenerative Medicine and Stem Cell Research, University of California–Los Angeles, Los Angeles, CA 90095, USA. [10]Crump Institute for Molecular Imaging, University of California–Los Angeles, Los Angeles, CA 90095, USA.
*Corresponding author. Email: owenwitte@mednet.ucla.edu (O.N.W.); tgraeber@mednet.ucla.edu (T.G.G.)

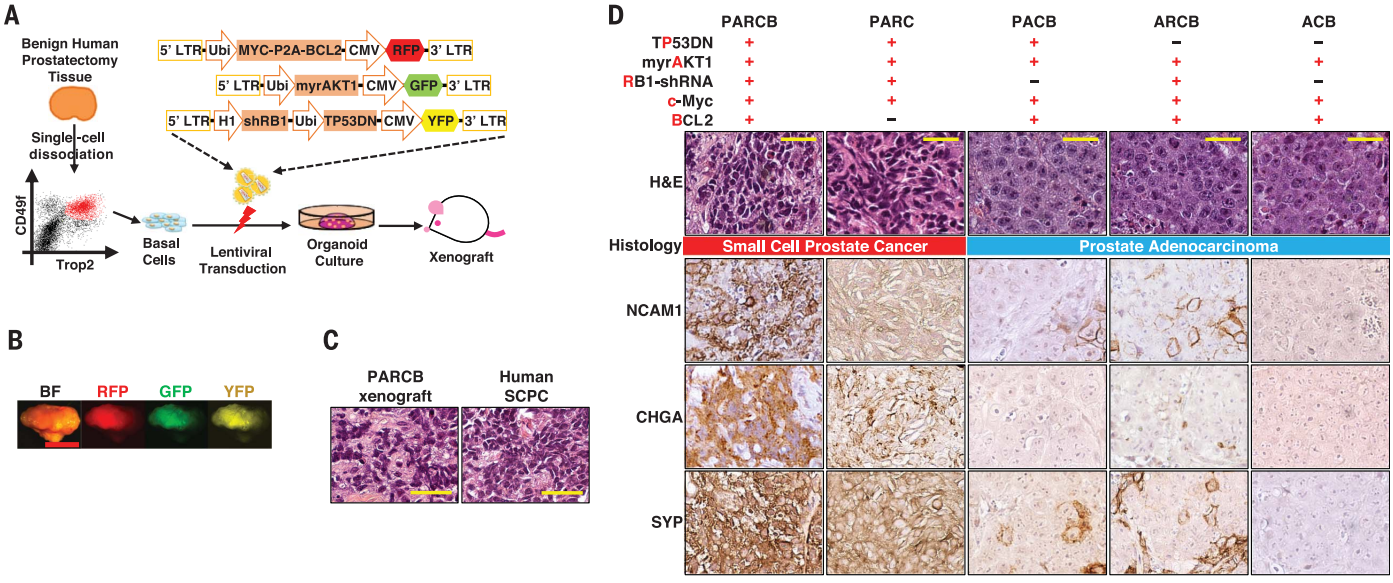


**Fig. 1. Defined genes drive human prostate epithelial cells to the SCPC phenotype.** (**A**) Schematic of human prostate transformation assay. LTR, long terminal repeats; CMV, cytomegalovirus promoter; Ubi, ubiquitin promoter. (**B**) Representative image of PARCB xenografts displaying GFP, RFP, and YFP expression. BF, bright field. Scale bar, 1 cm. (**C**) Hematoxylin and eosin (H&E)–stained images of PARCB grafts and human SCPC. Scale bars, 50 μm. (**D**) H&E staining and immunohistochemistry (IHC) images with antibodies against the indicated proteins in genetically engineered tumor models. Scale bars, 50 μm.

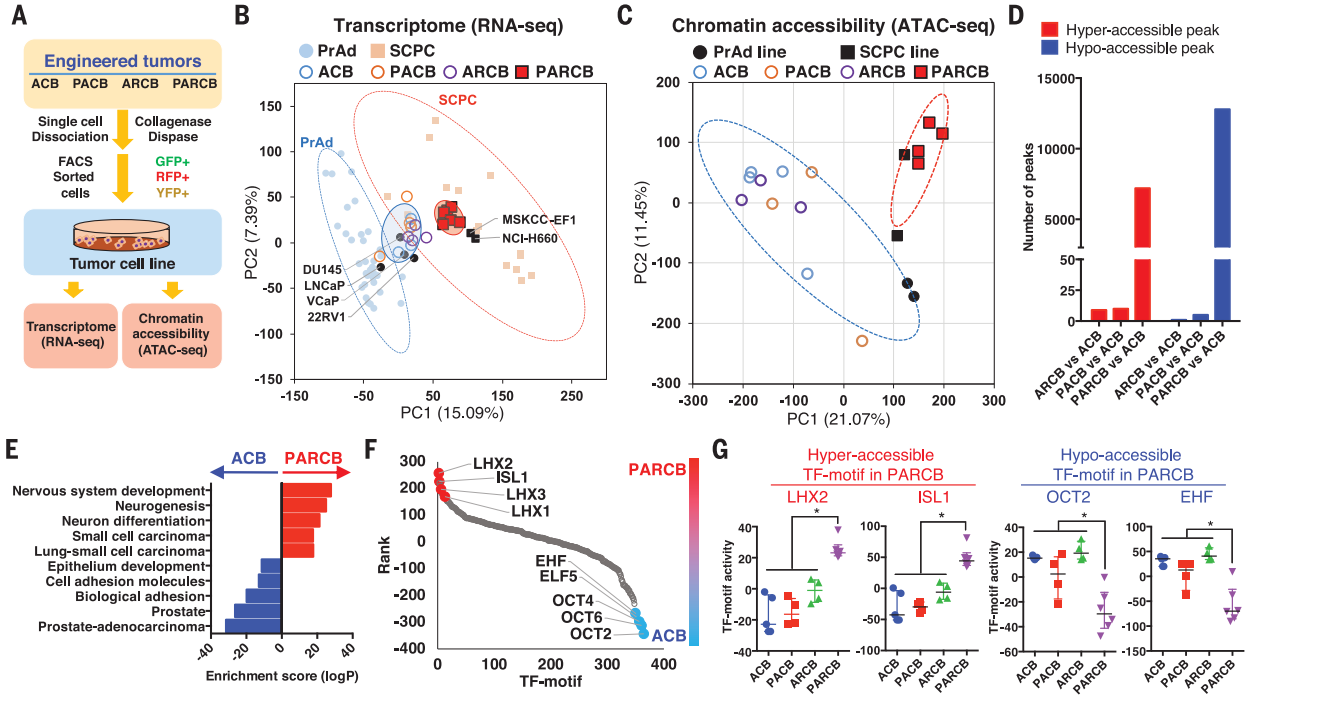


**Fig. 2. Inactivation of both p53 and RB is required to reprogram transcriptional profiles and chromatin accessibility landscapes of normal prostate epithelial cells to human SCPC.** (**A**) Schematic for establishment of tumor cell lines with GFP-, RFP-, and YFP-positive purified xenograft cells. (**B**) Partial least-squares regression analysis (PLSR) separates PrAd and SCPC specimens in the RNA-seq dataset from Beltran *et al*. (*7*). RNA-seq data for engineered tumor lines and patient-derived prostate cancer cell lines were projected onto the PLSR plot. (**C**) Principal components analysis (PCA) of ATAC-seq data from engineered cell lines with PrAd and SCPC lines. Probability ellipse = 95% confidence to group the samples. (**D**) Hyper- or hypo-accessible peaks in comparisons between engineered tumor lines. (**E**) Selected gene sets enriched in hyper- or hypo-accessible peaks in the comparison between PARCB and ACB lines. (**F**) TF binding motifs identified by HOMER (*34*) motif analysis were plotted by ranks generated from their associated differential adjusted *P* values. (**G**) Transcriptional activities of the TF motifs were measured by gene signature scores (see materials and methods). Medians with interquartile ranges are shown. **P* < 0.05 [one-way analysis of variance (ANOVA)].

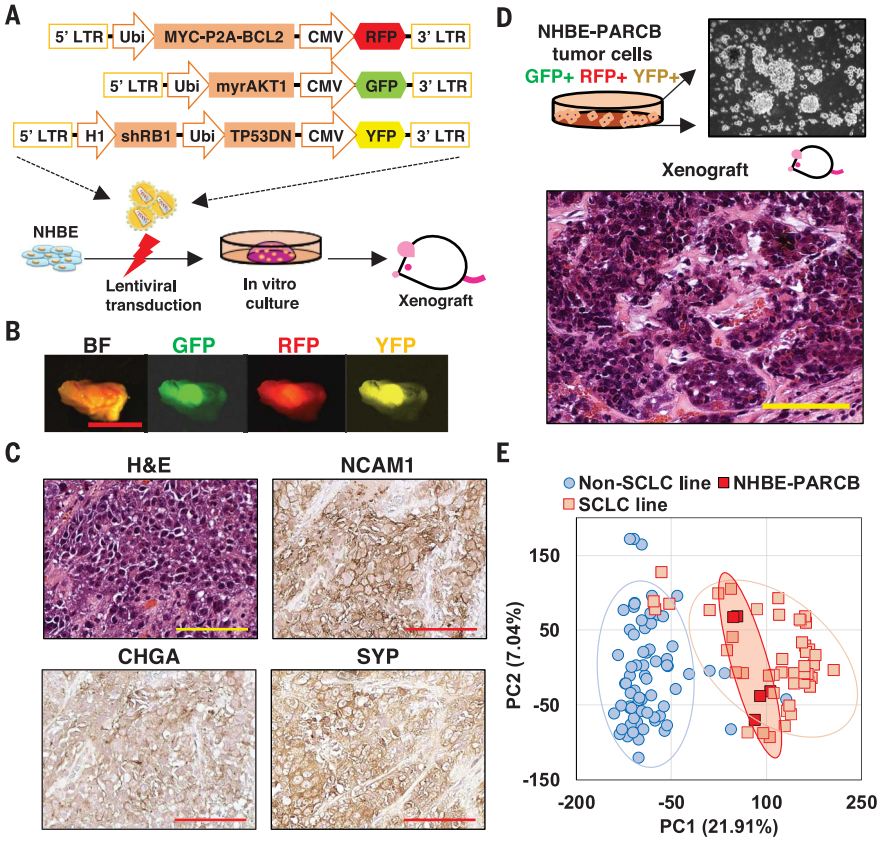


**Fig. 3. The same genetic drivers for SCPC can initiate SCLC from human normal lung epithelial cells.** (**A**) Schematic of NHBE cell transformation. (**B**) Representative tumor image displaying the lentivirally colinked markers GFP, RFP, and YFP. Scale bar, 1 cm. (**C**) H&E and IHC images against NED markers in transformed NHBE xenografts. Scale bars, 100 μm. (**D**) Representative morphologic image of NHBE-PARCB cell lines in two-dimensional culture and H&E image of xenografts derived from NHBE-PARCB cell lines. Scale bar, 100 μm. (**E**) PCA of NHBE-PARCB cell lines with SCLC and non-SCLC cell lines.

accessibility and its association with transcriptional programs by ATAC-seq. PARCB and patient-derived SCPC lines exhibited a distinct chromatin accessibility status compared with the ACB, PACB, or ARCB lines (Fig. 2C and fig. S4B). Dual inactivation of p53 and RB in PARCB lines induced marked changes in chromatin accessibility compared with that in ACB lines (Fig. 2D). However, single inactivation of p53 or RB alone in PACB or ARCB lines, respectively, did not alter chromatin accessibility compared with that in ACB lines (Fig. 2D).

Chromatin regions in PARCB lines that were hyperaccessible compared with those in ACB lines were highly enriched for genes associated with neuronal differentiation and small cell lung cancer (SCLC), whereas hypo-accessible regions in PARCB lines were enriched for epithelial development– and PrAd-associated genes (Fig. 2E). We conclude that concomitant p53 and RB disruption is required and may synergize to promote lineage plasticity during human prostate epithelial transformation by modulating transcriptional and epigenetic programs, supporting previous findings from mouse models (*8*, *19*).

To further characterize p53 and RB inactivation–induced changes in chromatin, we performed transcription factor (TF) binding motif enrichment analysis with the differentially accessible peaks in PARCB lines compared with ACB lines. We found that LHX family TF motifs (LHX1, LHX2, and LHX3) and ISL1 were the most accessible regions in PARCB lines, whereas OCT family TF motifs (OCT2 and OCT6) and ETS family TF motifs (EHF and ELF5) were less accessible in PARCB than in ACB lines (Fig. 2F and table S1). Although the biological functions of these TFs are unexplored in prostate cancer, we were able to assess the transcriptional activity of these TF motifs altered by concomitant p53 and RB disruption. Our integrated analysis with the matched RNA-seq data revealed that enriched accessibility of LHX2-, ISL1-, OCT2-, or EHF-DNA binding motifs was mirrored by the expression of the downstream target genes (Fig. 2G).

We next investigated how similar the PARCB lines might be to SCNCs from other organs. We performed a gene list enrichment analysis (*20*) of 938 transcriptionally profiled cancer cell lines by using genes up-regulated in the PARCB lines (table S2). This analysis demonstrated that the PARCB cell lines were transcriptionally most similar to SCLC cell lines and the NCI-H660 SCPC cell line (fig. S8 and table S3). To further evaluate the similarity of SCPC and SCLC, we projected gene expression data from human lung cancer samples [from (*21*) and The Cancer Genome Atlas (TCGA) (*22*)] onto our prostate cancer clustering plot in Fig. 2B. All clinical SCLC samples tightly clustered with the SCPC samples, indicating that prostate and lung SCNCs are both histologically and transcriptionally similar (fig. S9).

Given the similarity of the PARCB prostate cancer models to SCPC and SCLC, we next asked whether the PARCB factors could initiate SCLC from human lung epithelial cells. In a fashion similar to our transformation of primary human prostate cells, we transformed primary normal human bronchial epithelial (NHBE) cells with the PARCB lentiviruses (Fig. 3A). Xenografts (NHBE-PARCB) expressed GFP, RFP, and YFP (Fig. 3B) and the PARCB factors (fig. S10A). NHBE-PARCB tumors showed typical histological features and NED marker expression characteristic of clinical SCLC (Fig. 3C). Removing one gene from the PARCB combination did not result in tumor growth. Similar to clinical SCLC (*23*), all of the tumors expressed the proliferation marker Ki67 and none expressed the basal-squamous epithelial cell markers p63 and cytokeratin 14 (fig. S10B).

To interrogate the convergent evolutionary pattern of SCNCs, we established five NHBE-PARCB tumor cell lines for downstream multi-omics analyses. Like the prostate PARCB lines, the NHBE-PARCB lines propagated in suspension, demonstrated tumorigenic potential in vivo (Fig. 3D), and exhibited transcriptional similarity to patient-derived SCLC cell lines [from the Cancer Cell Line Encyclopedia database (*24*)] (Fig. 3E). Comparative genomic hybridization and whole-exome sequencing analyses identified no recurrent genetic alterations between prostate and lung PARCB models, indicating that the defined five genetic factors are likely sufficient to drive human SCNC (fig. S11 and tables S4 and S5).

We found that normal prostate basal epithelial cells and NHBE cells displayed distinct transcriptomes. In contrast, the prostate PARCB and NHBE-PARCB cell lines tightly clustered together, indicating a shared gene expression profile associated with reprogramming by the PARCB factors irrespective of the tissue of origin (Fig. 4A). We then examined transcriptome data from SCPC and SCLC patient biopsy specimens (*7*, *21*) and compared these with their respective adjacent normal tissues from TCGA. These results support the finding that SCPC and SCLC are transcriptionally convergent relative to the normal epithelial cells from which they originated (Fig. 4B) and demonstrate that a similar convergence occurs in patients.

Both transcriptional and epigenetic regulatory networks dictate cell lineage decisions (*25*, *26*). We investigated the nature of the global chromatin states involved in the convergent transformation to SCNC by ATAC-seq. PARCB, SCPC,

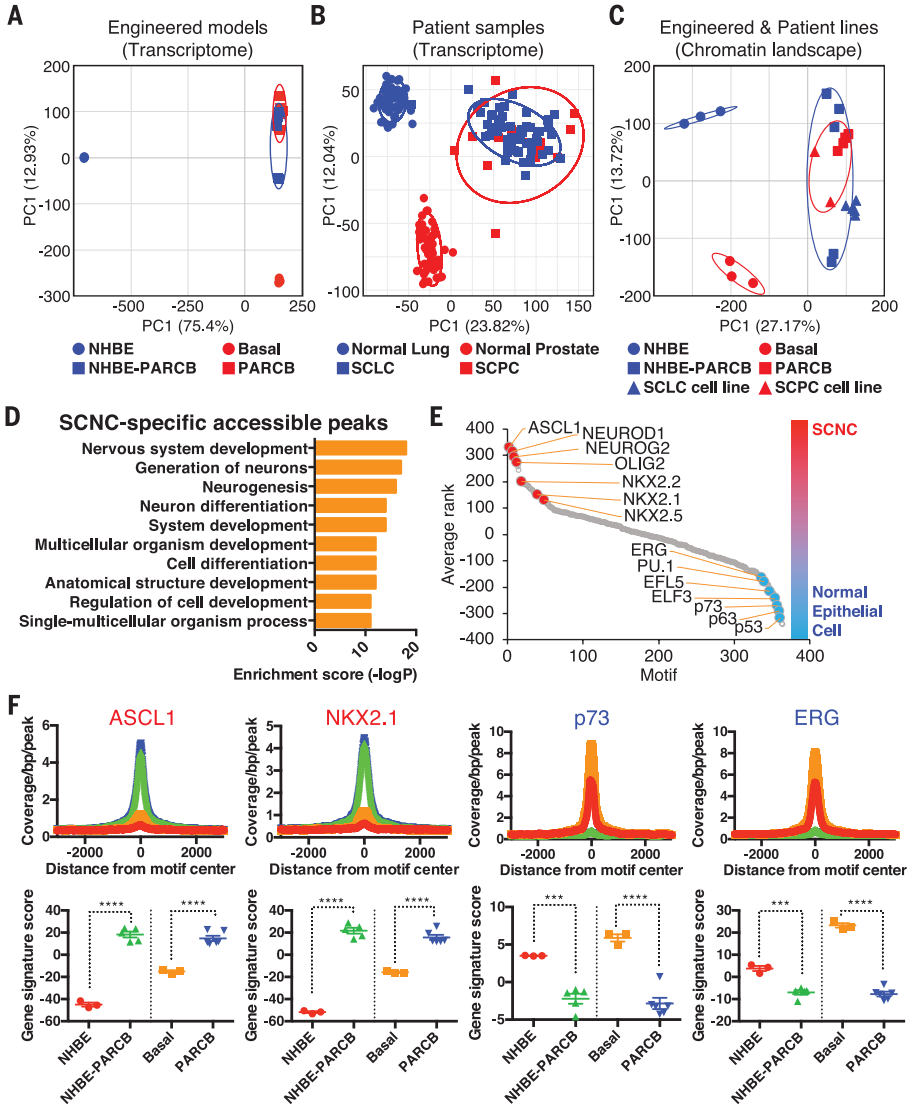


**Fig. 4. Convergent transcriptional and chromatin accessibility landscapes of SCPC and SCLC identify shared TF motifs.** (**A**) PCA of RNA-seq data from normal lung and prostate epithelial cells (NHBE and basal) and engineered lung and prostate PARCB cells. (**B**) PCA of RNA-seq data from human samples: SCLC and SCPC specimens and adjacent normal lung and prostate tissues. (**C**) PCA of ATAC-seq data from NHBE, basal, NHBE-PARCB, PARCB, and patient-derived SCLC and SCPC lines. (**D**) Gene Ontology terms for hyperaccessible peaks in lung and prostate SCNCs. (**E**) TF motifs identified by HOMER motif analysis were plotted by ranks generated from their associated differential *P* values (table S7). (**F**) (Top) Selected visualization of ATAC-seq footprint. bp, base pair. (Bottom) The transcriptional activities were measured by gene signature scores (see materials and methods). Medians with interquartile ranges are shown. ***$P < 0.001$, ****$P < 0.0001$ (one-way ANOVA).

and SCLC lines exhibited similar chromatin accessibility landscapes (Fig. 4C and fig. S12), which paralleled their transcriptional resemblance. Notably, the chromatin accessibility profiles of patient-derived SCPC and SCLC cell lines clustered with our prostate and NHBE-PARCB cell lines but not with non-neuroendocrine prostate and lung epithelial cells (Fig. 4C). We identified shared hyper- and hypo-accessible chromatin regions in the lung and prostate SCNCs compared with normal lung and prostate epithelial cells (fig. S13). The SCNC-specific accessible regions were enriched for genes important for development and neuronal differentiation (Fig. 4D and table S6).

To gain insight into the possible biological roles of TFs that serve as master regulators in SCNCs, we performed DNA binding motif enrichment analysis of the hyperaccessible regions. This analysis revealed motifs corresponding to proneural TFs (ASCL1, NEUROD1, NEUROG2, and OLIG2) and NKX homeodomain TFs (NKX2.1, NKX2.2, NKX2.5, and NKX6.1) (Fig. 4E and table S7). ASCL1 and NEUROD1 are required for SCLC survival and initiation (*27*–*29*). NEUROD1, NEUROG2, and NKX homedomain TFs are implicated in neural stem cell patterning and neural progenitor fate specification (*30*). NKX2.1/TTF-1 is a biomarker for SCLC and SCPC (*31*). We found that the chromatin regions for binding p53 family TFs (p53, p63, and p73) and ETS family TFs (ELF3, ELF5, and ERG) were less accessible in SCNCs than in normal epithelial cells (Fig. 4E). Both of these TF families also play critical roles in neuronal development and lineage decisions (*32*, *33*). Our motif analysis identified TFs known to be involved in neural proliferation and differentiation as well as additional TFs (table S7) with unexplored roles in SCNC. We next evaluated both RNA-seq and ATAC-seq data to compare the transcriptional activity of these TFs with the global accessibility of their DNA binding motifs. Our integrated analysis revealed that the differentially accessible TF motifs we identified correlated with the transcriptional output of TF target genes for each motif (Fig. 4F and fig. S14). These findings indicate that concomitant enrichment of proneural TFs and NKX homeodomain TFs and silencing of ETS family TF and p53 family TF transcriptional activities are conserved in and are likely critical for transformation to SCNC across tissue types.

Current therapeutic strategies designed to inhibit oncogenic pathways driving malignant phenotypes almost inevitably lead to treatment-resistant cancers. Increasingly, treatment-resistant tumors that assume aggressive clinical characteristics and molecular features of both stemlike and neuroendocrine lineages are being identified in a variety of epithelial cancers. We provide cellular, transcriptional, and epigenetic evidence that the SCNC phenotype that arises from distinct epithelial organs represents a common point in the evolution of cancers that is induced by shared genetic and epigenetic processes. Although normal human epithelial cells derived from developmentally distinct organs have their own molecular landscapes, our findings demonstrate that a defined set of oncogenic factors can induce the development of a common lethal neuroendocrine cancer lineage (SCNC) from different epithelial cell types. We have characterized the essential contribution of these factors and the convergence of both the transcriptional and chromatin landscapes during the process of transformation to SCNC. Our integrated molecular analyses have identified a group of key TFs that appear to be critical for the initiation and maintenance of SCNC, independently of the tissue of origin. These data may help inform efforts to identify novel therapeutic approaches for preventing the emergence of SCNCs and for treating them once they arise.

## REFERENCES AND NOTES

1. D. Hanahan, R. A. Weinberg, *Cell* **144**, 646–674 (2011).
2. R. Nadal, M. Schweizer, O. N. Kryvenko, J. I. Epstein, M. A. Eisenberger, *Nat. Rev. Urol.* **11**, 213–219 (2014).
3. A. F. Gazdar, P. A. Bunn, J. D. Minna, *Nat. Rev. Cancer* **17**, 765 (2017).
4. L. V. Sequist *et al.*, *Sci. Transl. Med.* **3**, 75ra26 (2011).
5. H. L. Tan *et al.*, *Clin. Cancer Res.* **20**, 890–903 (2014).

6. M. J. Niederst *et al*., *Nat. Commun.* **6**, 6377 (2015).
7. H. Beltran *et al*., *Nat. Med.* **22**, 298–305 (2016).
8. S. Y. Ku *et al*., *Science* **355**, 78–83 (2017).
9. R. Fisher *et al*., *Genome Biol.* **15**, 433 (2014).
10. H. Chen, X. He, *Mol. Biol. Evol.* **33**, 4–12 (2016).
11. N. McGranahan, C. Swanton, *Cell* **168**, 613–628 (2017).
12. T. Stoyanova *et al*., *Proc. Natl. Acad. Sci. U.S.A.* **110**, 20111–20116 (2013).
13. V. Parimi, R. Goyal, K. Poropatich, X. J. Yang, *Am. J. Clin. Exp. Urol.* **2**, 273–285 (2014).
14. J. K. Lee *et al*., *Cancer Cell* **29**, 536–547 (2016).
15. Y. Lin, J. Fukuchi, R. A. Hiipakka, J. M. Kokontis, J. Xiang, *Cell Res.* **17**, 531–536 (2007).
16. M. Krajewska *et al*., *Am. J. Pathol.* **148**, 1567–1576 (1996).
17. L. D. Shultz, F. Ishikawa, D. L. Greiner, *Nat. Rev. Immunol.* **7**, 118–130 (2007).
18. P. Mu *et al*., *Science* **355**, 84–88 (2017).
19. M. Zou *et al*., *Cancer Discov.* **7**, 736–749 (2017).
20. E. Y. Chen *et al*., *BMC Bioinformatics* **14**, 128 (2013).
21. J. George *et al*., *Nature* **524**, 47–53 (2015).
22. National Cancer Institute, The Cancer Genome Atlas; https://cancergenome.nih.gov/.
23. H. Zhang *et al*., *Mod. Pathol.* **18**, 111–118 (2005).
24. J. Barretina *et al*., *Nature* **483**, 603–607 (2012).
25. W. K. Cheung, D. X. Nguyen, *Oncogene* **34**, 5771–5780 (2015).
26. W. A. Whyte *et al*., *Cell* **153**, 307–319 (2013).
27. H. Osada, Y. Tatematsu, Y. Yatabe, Y. Horio, T. Takahashi, *Cancer Res.* **65**, 10680–10685 (2005).
28. T. Jiang *et al*., *Cancer Res.* **69**, 845–854 (2009).
29. J. K. Osborne *et al*., *Proc. Natl. Acad. Sci. U.S.A.* **110**, 6524–6529 (2013).
30. F. Guillemot, *Development* **134**, 3771–3780 (2007).
31. S. N. Agoff *et al*., *Mod. Pathol.* **13**, 238–242 (2000).
32. P. Remy, M. Baltzinger, *Oncogene* **19**, 6417–6431 (2000).
33. B.Joseph, O. Hermanson, *Exp. Cell Res.* **316**, 1415–1421 (2010).
34. S. Heinz *et al*., *Mol. Cell* **38**, 576–589 (2010).


## ACKNOWLEDGMENTS

We thank the University of California, Los Angeles (UCLA) Tissue Procurement Core Laboratories for tissue preparation and the UCLA Technology Center for Genomics and Bioinformatics for preparing for RNA-seq and ATAC-seq analyses. We thank Y. Chen at Memorial Sloan Kettering Cancer Center for sharing the MSK-PCa4 SCPC organoid cell line. **Funding:** J.W.P. is supported by a UCLA Broad Stem Cell Research Center postdoctoral fellowship and the National Institutes of Health/National Cancer Institute (NIH/NCI) grant K99/R00 Pathway to Independence award K99CA218731. J.K.L. is supported by a Prostate Cancer Foundation (PCF) Young Investigator award and a Department of Defense (DOD) Prostate Cancer Research Program-Physician Research award. B.A.S. is supported by a PCF Young Investigator award and an American Cancer Society postdoctoral fellowship award. K.M.S. is supported by the UCLA Medical Scientist Training Program (NIH NIGMS T32 GM008042). C.C. and S.K.K. are supported by NIH grant CA178415. J.H. is supported by National Cancer Institute grants 1R01CA172603-01A1 and 1R01CA205001-01. T.G.G. is supported by the NCI/NIH (P01 CA168585) and an American Cancer Society Research Scholar award (RSG-12-257-01-TBE). T.G.G. and O.N.W. are supported by the UCLA SPORE in Prostate Cancer (NIH P50 CA092131) and a grant from the Medical Research Grant Program of the W. M. Keck Foundation. O.N.W. is supported by the Eli and Edythe Broad Center of Regenerative Medicine and Stem Cell Research and the Hal Gaba Fund for Prostate Cancer Research. **Author contributions:** J.W.P., J.K.L., B.A.S., and O.N.W. designed the study and experiments. J.W.P., J.K.L., L.W., and K.N. prepared lentiviral constructs, performed human prostate and lung transformation assays, and prepared samples for RNA-seq and ATAC-seq. J.W.P., L.W., and K.N. performed immunostaining analyses. J.W.P., N.G.B., K.M.S., B.A.S., C.C., B.L.T., S.K.K., and T.G.G. contributed to designing and performed bioinformatics analyses with RNA-seq and ATAC-seq data. S.K.K. and T.G.G. supervised the bioinformatics analyses. D.C. and K.N. contributed to processing human tissues and performing FACS analysis. J.H., L.W., and K.N. performed histological analyses. O.N.W. supervised the research. J.W.P. and O.N.W. wrote the manuscript with input from all authors. **Competing interests:** O.N.W. is a Scientific Advisor for Kronos Bio, a company developing chemical modulators of TFs and other targets in oncology. **Data and materials availability:** The RNA-seq, ATAC-seq, and whole-exome shotgun sequencing data reported in this article have been deposited in NCBI GEO under accession number GSE118207.

## SUPPLEMENTARY MATERIALS

www.sciencemag.org/content/362/6410/91/suppl/DC1
Materials and Methods
Figs. S1 to S14
Tables S1 to S11
References (*35*–*50*)

14 March 2018; resubmitted 3 July 2018
Accepted 9 August 2018
10.1126/science.aat5749

# Reprogramming normal human epithelial tissues to a common, lethal neuroendocrine cancer lineage

Jung Wook Park, John K. Lee, Katherine M. Sheu, Liang Wang, Nikolas G. Balanis, Kim Nguyen, Bryan A. Smith, Chen Cheng, Brandon L. Tsai, Donghui Cheng, Jiaoti Huang, Siavash K. Kurdistani, Thomas G. Graeber and Owen N. Witte

*Science* **362** (6410), 91-95.
DOI: 10.1126/science.aat5749

**Some (re)programming notes on cancer**

Epithelial cancers develop resistance to targeted therapies in a number of different ways. Several cancer types do so by undergoing phenotypic conversion to a highly aggressive cancer called small cell neuroendocrine carcinoma (SCNC). Whether distinct cancer types accomplish this "reprogramming" through the same mechanism has been unclear. Park *et al.* show that the same set of oncogenic factors transforms both normal lung and normal prostate epithelial cells into SCNCs that resemble clinical samples (see the Perspective by Kareta and Sage). This convergence of molecular pathways could potentially simplify the development of new therapies for SCNC, which is currently untreatable.

*Science*, this issue p. 91; see also p. 30